RSC Advances

ROYAL SOCIETY OF CHEMISTRY

www.rsc.org/advances

Table of Contents

Exploring the catalytic activity of new water soluble dinuclear copper(II) complexes towards the glycoside hydrolysis

Shobhraj Haldar, Ayan Patra and Manindranath Bera*

Department of Chemistry, University of Kalyani, Kalyani, Nadia, West Bengal – 741235, INDIA.
E-mail:mbera2009@klyuniv.ac.in; Tel.:+91 33 25828282x306; Fax:+91 33 25828282

Water soluble dicopper(II/II) complexes of a new dinucleating ligand, H_3phpda were synthesized and characterized for the investigation of glycoside hydrolysis.

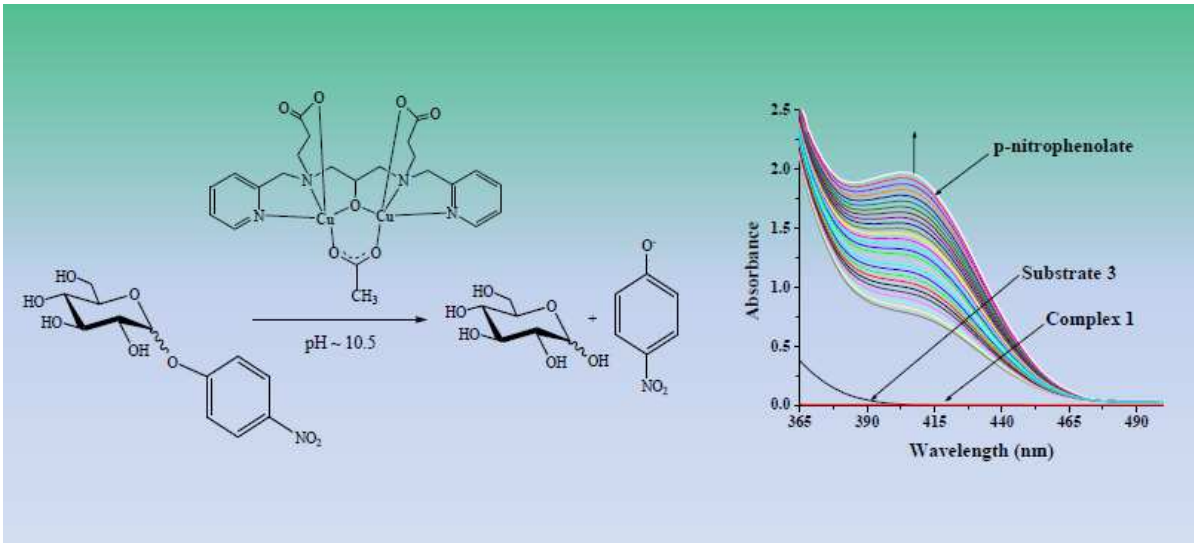

Exploring the catalytic activity of new water soluble dinuclear copper(II) complexes towards the glycoside hydrolysis

Shobhraj Haldar, Ayan Patra and Manindranath Bera*

Department of Chemistry, University of Kalyani, Kalyani, Nadia, West Bengal – 741235, INDIA.
E-mail:mbera2009@klyuniv.ac.in; Tel.:+91 33 25828282x306; Fax:+91 33 25828282

Abstract

Two water soluble dinuclear copper(II) complexes of a new dinucleating ligand, H_3phpda [H_3phpda = *N*,*N*′-bis(2-pyridylmethyl)-2-hydroxy-1,3-propanediamine-*N*,*N*′-dipropionic acid] have been synthesized and characterized for the investigation of catalytic hydrolysis of glycosides. In methanol, the reaction of stoichiometric amounts of $Cu(OAc)_2 \cdot H_2O$ and the ligand H_3phpda in the presence of NaOH, produced a new water soluble dinuclear copper(II) complex, $[Cu_2(phpda)(\mu\text{-}OAc)]$ (**1**). Similarly, the reaction of stoichiometric amounts of $Cu(ClO_4)_2 \cdot 6H_2O$ and the ligand H_3phpda in the presence of NaOH, in methanol, afforded a new water soluble dinuclear copper(II) complex, $[Cu_2(phpda)(H_2O)_2](ClO_4)$ (**2**). Characterizations of the complexes have been performed using various analytical techniques including DFT calculation. The DFT optimized structure of complex **1** shows that two copper(II) centers are in a distorted square pyramidal geometry with Cu---Cu separation of 3.677 Å. On the other hand, the DFT optimized structure of complex **2** reveals that one copper(II) center adopts a five-coordinate distorted square pyramidal geometry and the other copper(II) center is in a distorted square planar geometry with Cu---Cu separation of 3.553 Å. Further, the mass spectroscopic analyses of complexes **1** and **2** reconfirm their dimeric nature, even in solution. Glycosidase-like activity of complexes **1** and **2** has been evaluated in aqueous solution at pH~10.5 by UV-vis spectrophotometric technique using *p*-nitrophenyl-α-D-glucopyranoside and *p*-nitrophenyl-β-D-glucopyranoside as the model substrates. Both the two complexes are active in catalyzing the hydrolysis of glycosides. DFT calculation has been performed to find the Fukui functions at the metal centers in complexes **1** and **2** to predict the possible metal sites involved in the binding process with substrates during the catalytic hydrolysis reactions.

Introduction

Glycoside hydrolases encompass a large class of enzymes that catalyze the hydrolysis of glycosidic linkages. These enzymes which are prevalent in carbohydrate metabolism can be classified into a number of subfamilies based on the structural similarities. The structural and mechanistic details for these enzyme systems are available in the literature.[1-3] Several artificial enzymes mimic the glycoside hydrolysis to model the glycosyl transfer reactions observed in Nature and hence, these reactions are considerably important in the biological systems.[4-9] Synthesis of different carbohydrate entities can be achieved by the application of such glycosyl transfer reactions. Usually, a glycosyl transfer reaction is conveniently accomplished by glycosyl transferases, but the limited availability of these enzymes hampers their uses.[10] Glycosidases can be employed as substitutes, but they lack the selectivity and provide low reaction yields. Extensive research aimed at overcoming these problems using artificial enzyme mimics have been employed using cyclodextrins derivatized with dicyanohydrins,[5,8] diacids,[9] or trifluoromethyl groups.[4] Although, these catalysts show many enviable properties as functional enzyme mimics, they require elevated temperatures for their catalytic activities,[7] and have a propensity to decompose during the reaction. Besides, these catalysts are deficient in the catalytic activity when altering the model substrate from a *p*-nitrophenyl-glycoside to a *o*-nitrophenyl glycoside.[6,9] Using various metal ions such as Cu^{II}, Ni^{II}, Co^{II}, and Al^{III}, the efficient cleavage of some glycosides and disaccharides has been investigated,[11,12] but these systems, however, contract the pool of substrates to glycosides with strong metal ligating properties and excludes many naturally occurring glycosides such as disaccharides and oligosaccharides. Striegler and co-workers have recently contributed immensely to the field of supramolecular glycosidase mimics.[13-16] In this perspective, the other catalytic systems with wider applicability are essentially required.

The coordination behavior of the various dinucleating ligands containing alkoxo and carboxylato donor groups which are capable of binding two metal ions through direct bond formation to yield dinuclear metal complexes has been studied extensively.[17-19] Dinuclear metal complexes have been recognized at the active sites of many metalloenzymes.[20] Practically, the enzyme models are of enormous importance for the development of efficient molecular catalysts for organic reactions and of theoretical importance in elucidating the mechanisms of enzymatic reactions.[21] Therefore, the model studies with simple dinuclear metal complexes are becoming

more and more important in understanding biological functions of the dimetallic cores.[22] Generally, in a dimetallic system, one metal ion is responsible for substrate binding while the other delivers the activated solvent nucleophile for hydrolysis. The dinuclear copper(II) complexes with either one loosely bound apical exogeneous ligand or coordinatively unsaturated ligand, have the potential for binding of biologically important substrates, thereby providing new reactivity patterns. So, the dinuclear copper(II) complexes with two metal ions in close proximity have received considerable attention as structural models for glycoside hydrolases which catalyze the hydrolysis of various glycosides.[13-16] The focus of this paper is on a new dinucleating ligand, *N*,*N*′-bis(2-pyridylmethyl)-2-hydroxy-1,3-propanediamine-*N*,*N*′-dipropionic acid (H_3phpda), incorporating two propionate and two pyridine functionalities and its coordination ability to bind two divalent copper(II) ions. Presently, we report the synthesis, characterization, spectroscopic details and the catalytic activity towards the glycoside hydrolysis of two new water soluble dinuclear copper(II) complexes.

Results and discussion

Syntheses and characterization

The new symmetrical dinucleating ligand, H_3phdpa has been synthesized in two step reactions as shown in Scheme 1. The synthesis of the precursor ligand, 2-hydroxy-1,3-propanediamine-*N*,*N*′-dipropionic acid (H_3hpda) has been accomplished by the reaction of stoichiometric amounts of 1,3-dichloro-propan-2-ol and β-alanine in the presence of LiOH in aqueous medium under stirring condition at ~ 40°C for 3 days. Acidification of the resulting solution by addition of HBr to pH~5 produced an off-white solid product. The product has been characterized to be the precursor ligand, H_3hdpa by different analytical techniques such as elemental analysis, FTIR and NMR spectroscopy. Alkylation of the secondary amines of H_3hdpa with stoichiometric quantities of 2-picolylchloride hydrochloride yielded the dinucleating ligand, H_3phpda, in good yield. The ligand H_3phpda has been fully characterized using the techniques such as elemental analysis, FTIR (Fig. S1, Supporting Information), NMR (Fig. S2 and Fig. S3, Supporting Information) and ESI mass (Fig. S4, Supporting Information) spectroscopy.

The dinucleating ligand, H_3phdpa containing two carboxylate functionalities and two pyridine arms has been chosen for this investigation because the metal complexes under such coordination environments were found to be highly water soluble, which has allowed us to study

the glycoside hydrolysis reactions in aqueous solution. In addition, the central pendant alcoholic arm of the ligand acts as a spacer-cum-bridging unit between two copper(II) ions in the Cu_2 complex.

The reaction of the ligand H_3phpda with $Cu(OAc)_2 \cdot H_2O$ in 1:2 molar ratio in the presence of a strong base, NaOH in methanol formed a bluish green dinuclear complex, $[Cu_2(phpda)(\mu\text{-}OAc)]$ (**1**) (Scheme 2). Similarly, the reaction of ligand H_3phpda with $Cu(ClO_4)_2 \cdot 6H_2O$ in 1:2 molar ratio in the presence of NaOH in methanol produced a green dinuclear complex, $[Cu_2(phpda)(H_2O)_2](ClO_4)$ (**2**) (Scheme 2). The complexes **1** and **2** are fully characterized by the elemental analysis, solution molar electrical conductivity, room temperature magnetic moment, FTIR, UV-vis, mass and EPR spectroscopic analyses. The molar conductivity value of complex **1** in MeOH is 37 $ohm^{-1}cm^2mol^{-1}$ at room temperature, indicating a non-electrolytic formulation.[23] However, the molar conductivity value of complex **2** in MeOH is 105 $ohm^{-1}cm^2mol^{-1}$ at room temperature, indicating a behavior attributable to 1:1 electrolyte.[23] The solid state room temperature magnetic moment values per copper for complexes **1** and **2** are 1.65 μ_B and 1.60 μ_B, respectively, indicating the occurrence of a strong antiferromagnetic coupling between the ligand bridged copper(II) ions in both the two complexes.

Spectroscopic studies of the complexes

The different modes of carboxylate coordination, specifically, monodentate terminal coordination of propionate groups of the ligand in both complexes **1** and **2** and *syn-syn* bidentate bridging coordination of exogeneous acetate group in complex **1** have been indicated by the FTIR spectra of the complexes. In the FTIR spectra of complex **1** (Fig. S5, Supporting Information), two strong asymmetric ν_{as} (COO^-) vibrations were observed at 1605 and 1568 cm^{-1} and two strong symmetric $\nu_s(COO^-)$ vibrations were observed at 1416 and 1345 cm^{-1}. The significantly higher difference, Δ ($\Delta = \nu_{as}(COO^-) - \nu_s(COO^-)$) of ~260 cm^{-1} between the asymmetric and symmetric stretching vibrations is attributed to the monodentate terminal coordination of propionate funtionalities.[24] The lower value of Δ at ~152 cm^{-1} between the asymmetric and symmetric stretching vibrations is characterized by the *syn-syn* bidentate bridging ($\eta^1{:}\eta^1{:}\mu_2$) of the exogenous acetate group.[24] The characteristic propionate bands at 1609 and 1336 cm^{-1} correspond to a strong asymmetric stretching frequency and a strong symmetric stretching frequency, respectively, which are observed in the FTIR spectra of complex **2**. The

significantly higher value of Δ at ~273 cm^{-1} frequently indicates the monodentate terminal coordination of the carboxylate group.[24] The FTIR spectra of complexes **1** and **2** also exhibit a broad absorption at ~3432 cm^{-1} typical of the *ν*(O-H) band from the coordinated or uncoordinated water molecules. In addition, a strong band (ν_{ClO4-}) at ~1088 cm^{-1} was observed in the FTIR spectra of complex **2** suggesting the presence of perchlorate ion outside the coordination sphere.[25]

The electronic spectra of complexes **1** and **2** in aqueous solution at pH~7.2 show a broad absorption band at 704 nm (ε, 115 $M^{-1}cm^{-1}$) and 706 nm (ε, 166 $M^{-1}cm^{-1}$), respectively, due to the d-d transition [Fig. S6(a) and Fig. S7(a), Supporting Information]. The spectra also display a distinct copper(II) ion bound ligand-based charge transfer transition at 257 nm (ε, 6155 $M^{-1}cm^{-1}$) and 258 nm (ε, 9522 $M^{-1}cm^{-1}$), respectively [Fig. S6(b) and Fig. S7(b), Supporting Information]. Again, the complexes are investigated for the catalytic activity towards the glycoside hydrolysis reactions in solution at pH ~10.5. In view of that, we have checked their stability and possibility of OH^- ion coordination at such a high pH, by running the electronic spectra of the complexes in aqueous solution at pH~10.5. The electronic spectra [Fig. S8(a) and Fig. S8(b), Supporting Information] of complexes **1** and **2** display a broad absorption band at 689 nm (ε, 71 $M^{-1}cm^{-1}$) and 688 nm (ε, 58 $M^{-1}cm^{-1}$), respectively, which are quite blue shifted from the spectra obtained at pH~7.2. Moreover, no precipitate of copper(II) hydroxide has been found at pH~10.5. Therefore, from the above observations, it can be suggested that the dinuclear complexes are stable in spite of the possibility of OH^- ion coordination in solution at pH~10.5.

The complexes **1** and **2** are EPR silent at room temperature both in solid state and in methanol solution. This is most possibly due to the strong antiferromagnetic coupling between the two copper(II) centers as revealed from their solid state room temperature magnetic susceptibility measurements. This behavior is observed in the literature for similar type of alkoxo bridged dinuclear copper(II) complexes.[26-29] In general, the alkoxo bridged dinuclear copper(II) complexes having Cu-$O_{bridging\ alkoxo}$-Cu bond angle ≥ 103° show strong antiferromagnetic behavior.[30,31]

In order to further characterize using ESI mass spectroscopic technique, the aqueous solutions of complexes **1** and **2** at pH~7.2, were positive-ion electrosprayed into a quadrupole ion-trap mass spectrometer and subjected to collision-induced dissociation to gain the structural informations. The mass spectrum of complex **1** (Fig. S9, Supporting Information) exhibits a

signal at *m/z* = 672 that corresponds to the $\{[Cu_2(phpda)(OAc)]\cdot 4H_2O+H\}^+$ species, confirming the dimetallic nature of complex **1** in solution. The mass spectrum of complex **2** (Fig. S10, Supporting Information) indicates a signal at *m/z* = 659 that corresponds to the $\{[Cu_2(phpda)(H_2O)(ClO_4)]+H\}^+$ species, confirming the dimetallic nature of complex **2** in solution. Again, keeping in mind that catalytic hydrolysis of glycosides is carried out in solution at pH ~10.5, ESI mass spectra were obtained on the aqueous solutions of complexes **1** and **2** at such high pH. The mass spectrum of complex **1** (Fig. S11, Supporting Information) displays the signals at *m/z* = 608 and 576 that match to the $\{[Cu_2(phpda)(H_2O)(OH)]\cdot CH_3OH+H\}^+$ and $\{[Cu_2(phpda)(H_2O)(OH)]+H\}^+$ species, respectively, confirming its dimetallic nature in spite of the possibility of OH^- ion coordination in solution at pH~10.5. Similarly, the mass spectrum of complex **2** (Fig. S12, Supporting Information) shows the signals at *m/z* = 594 and 576 that match to the $\{[Cu_2(phpda)(H_2O)(OH)]\cdot H_2O+H\}^+$ and $\{[Cu_2(phpda)(H_2O)(OH)]+H\}^+$ species, respectively, confirming the dimetallic nature of complex **2**, in spite of the possibility of OH^- ion coordination in solution at pH~10.5. Moreover, the mass spectroscopic results at pH~10.5 indicate that for both complexes **1** and **2**, the most possible active species responsible for the catalytic hydrolysis is $[Cu_2(phpda)(OH)(H_2O)]$.

Description of DFT optimized structures of complexes 1 and 2

Despite of our great efforts, we did not succeed in the preparation of single crystals of satisfying size of complexes **1** and **2**. So, the DFT calculation has been carried out to optimize the molecular structures of the complexes to find the intermetallic distances and overall geometry of the copper(II) centers. Views of the DFT optimized structures are depicted in Fig. 1 and Fig 2. Selected bond lengths and bond angles are given in Table 1 and Table 2. Both the structures reported here were optimized without any symmetry restrictions. The vibrational frequencies were analyzed to confirm the identity of the stationary point and it was found to be a minimum (without any negative frequency).

$[Cu_2(phpda)(\mu\text{-}OAc)]$ (1). The DFT optimized structure reveals that both the copper(II) centers exhibit a five-coordinate distorted square pyramidal geometry with trigonality factor (τ) 0.223 and 0.338.[32] The square pyramidal geometry around Cu(1) center is described by the O(1), O(6), O(5) and N(1) atoms at the equatorial position and the N(4) atom at the axial position. Similarly,

square pyramidal geometry around Cu(2) center is defined by the O(3), O(7), N(3) and N(2) atoms at the equatorial position and the O(1) atom at the axial position. The exogenous acetate group binds two copper(II) ions in μ-*syn*-*syn*-η1:η1-fashion. This type of *syn*-*syn* bidentate bridging of carboxylate is common in dicopper complexes.[33-35] The Cu-$O_{bridging\ acetate}$ bond distances indicate that these bridges are close to symmetric [Cu(1)-O(6), 1.931 Å; Cu(2)-O(7), 1.965 Å]. The Cu-$O_{bridging\ alkoxo}$ bond distances [Cu(1)-O(1), 1.911 Å; Cu(2)-O(1), 2.095 Å] and Cu-$O_{bridging\ alkoxo}$-Cu bond angle [Cu(1)-O(1)-Cu(2) = 133.14°] fall in the range found for similar alkoxo bridged dinuclear copper(II) complexes.[36,37] The equatorial bond lengths around the copper(II) centers are in the range of 1.911-2.117 Å. The Cu(1)-N(4) and Cu(2)-O(1) axial bond lengths are 2.291 Å and 2.095 Å, respectively. The equatorial and axial bond lengths are in the range of those previously reported in the literature.[38-40] The two aliphatic carboxylate arms of the ligand are *cis* to each other with respect to the monodentate terminal binding of carboxylates. The Cu---Cu separation in the dinuclear unit is 3.677 Å which is comparable to those reported in the literature. [19a, 41,42]

$[Cu_2(phpda)(H_2O)_2](ClO_4)$ (2). The DFT optimized structure complex **2** consists of a monocationic species $[Cu_2(phpda)(OH_2)_2]^+$ and one ClO_4^- ion as the counter anion. The two copper(II) ions within the the Cu_2 unit are bridged by the central alkoxo oxygen atom of the ligand $phpda^{3-}$. Whereas, one copper(II) center displays a five-coordinate distorted square pyramidal geometry, the other copper(II) center shows a four-coordinate distorted square planar geometry. The square pyramidal geometry around Cu(1) center is defined by the O(1), O(7), N(4) and N(2) atoms at the equatorial position and the O(5) atom at the axial position. Similarly, the square planar geometry around Cu(2) center is completed by the O(1), O(6), O(3) and N(1) atoms. The Cu-$O_{bridging\ alkoxo}$ bond distances are within the range of previously reported alkoxo bridged dinuclear copper(II) systems at ~1.917 Å.[38-40] The Cu-O_{aqua} bond distances are within the range of values previously reported in the literature.[41-43] The Cu-$O_{bridging\ alkoxo}$-Cu bond angle [Cu(1)-O(1)-Cu(2) = 135.86°] is within the range of similar alkoxo bridged dinuclear copper(II) complexes reported in the literature.[36,37] The DFT optimized structure also reveals that the dinuclear Cu_2 unit presents *cis* arrangement of two aliphatic carboxylate arms of the ligand. The Cu---Cu separation in complex **2** is 3.553 Å which is comparable to the values reported in the literature.[19a,44,45] More interestingly, the DFT optimized structure of complex **2** features that one

2-methylpyridyl group at the half end of the ligand phpda^{3-} remains uncoordinated to the Cu(2) center. This selection seems to be reasonable because the nitrogen atom of this 2-methylpyridyl group is far away (~2.681 Å) from the Cu(2) center situated on the square plane. This is most possibly due the steric crowding among the uncoordinated 2-methylpyridyl group and coordinated propionate functionality and exogeneous water molecule which do not further allow the 2-methylpyridyl group to come to the bonding distance. A similar non-coordinating behavior of a pendant 2-methylpyridyl group of a dinucleating ligand has been observed in a bis(μ-alkoxo) bridged dinuclear vanadium(III) complex.[46]

Glycoside hydrolysis and kinetics

Catalytic hydrolysis of glycosidic linkages by glycoside hydrolases is shown in the Scheme 3. In sequence to evaluate the ability of complexes **1** and **2** to cleave glycosidic bonds, the hydrolysis of *p*-nitrophenyl-α-D-glucopyranoside and *p*-nitrophenyl-β-D-glucopyranoside was examined in aqueous solution in 50 mM CAPS buffer at pH~10.5. For this purpose, 1.0 x 10^{-5} M solutions of these complexes were treated with 2.0 x 10^{-4} M solutions of glycoside substrates separately, at room temperature under aerobic conditions. The course of the reaction was followed by UV-vis spectroscopic technique. After addition of each substrate to solutions of complexes **1** and **2**, a gradual increase in the band that corresponds to *p*-nitrophenolate was observed at 410 nm, as displayed in the UV-vis spectra (Fig. 3 and Fig. 4).

The kinetics of the hydrolysis of *p*-nitrophenyl-α-D-glucopyranoside and *p*-nitrophenyl-β-D-glucopyranoside were determined by the Michaelis-Menten approach of enzymatic kinetics by monitoring the increase of *p*-nitrophenolate band at 410 nm as a function of time. The concentration of each of the glycoside substrates was always kept at least 10 times larger than that of the catalysts to maintain the pseudo-first-order reaction condition. The dependence of the initial rate on complex and substrate concentration was studied in order to explicate the reactivity. As observed, the reaction was found to depend linearly on the catalyst concentration following the first order kinetics. Again, to determine the dependence of the rates on the substrate concentration and various kinetic parameters, the solutions of complexes **1** and **2** were treated with different concentrations of each glycoside substrate under aerobic conditions. At low concentrations of substrate, a first-order dependence on the substrate concentration was observed, but at higher concentrations, saturation kinetics were observed for both the complexes.

The Michaelis-Menten approach has also been applied to get the Lineweaver-Burk (double reciprocal) plot using the equation $1/V = (K_M/V_{max})\ (1/[S]) + 1/V_{max}$ as well as the values of the various kinetic parameters K_{cat}, K_M, V_{max} and K_{cat}/K_M which are reported in Table 3. The observed rate versus substrate concentration plots and the Lineweaver-Burk plots for complexes **1** and **2** are shown in Figs. 5, 6, 7 and 8. The turnover rates (K_{cat}) for complexes **1** and **2** with respect to *p*-nitrophenyl-α-D-glucopyranoside are 33.0 x 10^{-3} and 29.9 x 10^{-3} min^{-1}, respectively, and with respect to *p*-nitrophenyl-β-D-glucopyranoside are 8.6 x 10^{-3} and 53.7 x 10^{-3} min^{-1}, respectively, which are comparatively higher than the values for some dinuclear copper complexes reported in the literature.[13,14] The hydrolysis of glycoside substrates **3** and **4** in aqueous solution under the similar experimental conditions but in the absence of any catalyst is reported in the literature.[13] Hence, we have calculated an acceleration (K_{cat}/K_{non}) of the substrate hydrolysis and it has been found that the complexes **1** and **2** are able to cleave the glycosidic bond in substrates **3** and **4** with an average acceleration of the hydrolysis of up to 12.6 x 10^4 fold over the background reaction.

The control experiments have been performed under the similar experimental conditions to examine the hydrolysis of glycoside substrates **3** and **4** using free copper(II) acetate monohydrate and copper(II) perchlorate hexahydrate. Clearly, it has been found that the hydrolysis of the substrates is not promoted by the copper(II) acetate or perchlorate solution, as a precipitate (presumably Cu(II) hydroxide) is observed at pH~10.5.

The experimental data reported here allocate some preliminary conclusions on the possible mechanism of the glycoside hydrolysis promoted by the complexes **1** and **2**. The hydrolysis of the glycosides is linearly dependent on the catalyst concentration for both the complexes under the conditions employed. Nevertheless, an increase of the rate for the product formation is observed during the prolonged reaction time. It has also been observed that the *p*-nitrophenolate product does not deactivate the catalytic activity of the complexes, even during a 30 h time period at pH~10.5. The complexes may reorganize upon substitution of the coordinated sugar with water and subsequent proton loss in aqueous alkaline solution.

A comparison of the glycosidase activity of complexes **1** and **2** with respect to the substrates **3** and **4** can be made by rationalizing the data obtained from the Lineweaver-Burk plots. The turnover rates (K_{cat}) for complexes **1** and **2** with respect to the glycoside substrate **3** are comparable as their K_{cat} values are fairly close in magnitude, but the overall catalytic

efficiency of complex **1** (K_{cat}/K_m = 95.1 $M^{-1}min^{-1}$) to promote the hydrolysis of substrate **3** is considerably higher than that of complex **2** (K_{cat}/K_m = 8.7 $M^{-1}min^{-1}$). On the other hand, the turnover rate for complex **2** is much higher than that of complex **1** with respect to the glycoside substrate **4**, although the overall catalytic efficiency of complex **1** (K_{cat}/K_m = 27.7 $M^{-1}min^{-1}$) to promote the hydrolysis of substrate **4** is higher than that of complex **2** (K_{cat}/K_m = 7.3 $M^{-1}min^{-1}$). Considering the overall catalytic efficiency, the complex **1** is a better catalyst than complex **2** towards the hydrolysis of both *p*-nitrophenyl-α-D-glucopyranoside (**3**) and *p*-nitrophenyl-β-D-glucopyranoside (**4**) in aqueous alkaline solution. To the best of our knowledge, only a very few studies on glycoside hydrolysis by dinuclear copper complexes in aqueous alkaline solution have been reported in the literature.[13-16.] The K_{cat} values of these complexes at the respective pH optima (pH~10.5) make it clear that the complexes **1** and **2** are comparably better catalysts and they bind the glycoside substrates during catalysis much more strongly as observed from their K_m values (Table 3) and hence show higher overall catalytic efficiency.

The intermetallic distances in the dinuclear complexes **1** and **2** are comparable (~ 3.615 Å) as revealed by the discussion on their DFT optimized structural analyses. The observed difference in the catalytic performance of the complexes is therefore associated with the electronic features of the exogeneous ligand backbones as well as the influence of an overall geometry on the Lewis acidity of the copper(II) centers. The geometrical symmetry between the two copper(II) centers in complex **1** more possibly enhances the overall catalytic efficiency compared to that in case of the geometrical asymmetry between the two copper(II) centers in complex **2**.

DFT calculations

Theoretical calculations have been carried out to get a better understanding about the binding process of glycoside substrates with complexes **1** and **2** during the catalytic hydrolysis reactions. Calculations have been done on the neutral species $[Cu_2(phpda)(\mu\text{-}OAc)]$ (**1**) and cationic species $[Cu_2(phpda)(H_2O)_2]^+$ (**2**) and on the corresponding one-electron reduced analogues $\mathbf{1}^-$ and $\mathbf{2}^-$ at the B3LYP level using the Gaussian 03 software package. The calculated condensed Fukui function values f_k^+ at the copper centers of complexes **1** and **2** are given in Table 4. According to the values presented in Table 4, it can be indicated that the glycoside substrate binds as nucleophile to Cu(2) center (f_k^+ = 0.0970) more favorably than Cu(1) center (f_k^+ = 0.0167) in

complex **1**. Similarly, from the Fukui function values of complex **2**, it can be clearly believed that the glycoside substrate binds to Cu(1) center ($f_k^+ = 0.1739$) more favorably than Cu(2) center ($f_k^+ = 0.0147$). The relatively small difference in the Fukui function values at the two copper sites in complex **1** is most likely due to the different distortions in their square pyramidal coordination geometry. In contrast, the large difference in the Fukui function values at the two copper sites in complex **2** is most possibly due to the different coordination geometry around the two copper centers. Therefore, theoretical calculations strongly suggest that the substrate **3** and **4** will prefer to interact as nucleophile during the catalytic hydrolysis with one copper center in both complexes **1** and **2**. A representative proposed mechanism for the hydrolysis of *p*-nitrophenyl-α-D-glucopyranoside (**3**) by complex **1** showing the possible binding mode of substrate is given in the Scheme 4, based on the results obtained from electronic spectra, mass spectra and theoretical calculations. Recently, the similar binding events of different monosaccharides with dinuclear copper(II) complexes in aqueous alkaline solution have been reported in the literature.[47-49]

Conclusions

In the present work, the synthesis and characterization of two new water soluble dinuclear copper(II) complexes of a symmetrical dinucleating ligand holding two carboxylate functionalities and two pyridine arms have been reported. The DFT optimized structural analyses and spectroscopic investigations authenticated the dimetallic nature of complexes **1** and **2**. The complexes uphold the average copper-copper separation of 3.615 Å which is the optimum cooperativity between the two metal centers for mimicking the structural and functional models to the active site of glycoside hydrolase. In a simulated metal-metal distance and N_2O_3 coordination environment, both the complexes show moderate glycosidase like activity in aqueous alkaline solution. The catalytic efficiency of complex **1** (K_{cat}/K_m = 27.7 $M^{-1}min^{-1}$) is reasonably higher than that of complex **2** (K_{cat}/K_m = 7.3 $M^{-1}min^{-1}$) towards the hydrolysis of *p*-nitrophenyl-α-D-glucopyranoside and *p*-nitrophenyl-β-D-glucopyranoside. Density Functional Theory (DFT) calculations strongly suggest that during the catalytic hydrolysis, the binding of substrate with the dinuclear metal complexes **1** and **2** takes place more possibly through the involvement of one copper center. The present investigations will positively provide valuable insights and direction for the future design of water soluble transition metal complexes for the hydrolysis of various glycosides and hence, for the synthesis of non-natural carbohydrate entities.

Experimental section

Materials

2-picolylchloride hydrochloride, *p*-nitrophenyl-α-D-glucopyranoside and *p*-nitrophenyl-β-D-glucopyranoside were purchased from Sigma-Aldrich Chemie GmbH, Germany. β-alanine and 1,3-dichloro-2-propanol were purchased from SRL, India. Copper(II) acetate monohydrate was purchased from Merck, India. Copper(II) perchlorate hexahydrate was prepared by treating copper(II) carbonate with 1:1 perchloric acid and crystallized after concentrating on water bath. All other chemicals and solvents were reagent grade materials and were used as received without further purification.

Physical measurements

Microanalyses (C, H, N) were performed using a Perkin-Elmer 2400 CHNS/O Series II elemental analyser. FTIR spectra were obtained on a Perkin-Elmer L120-000A spectrometer (200-4000 cm^{-1}). The solution electrical conductivity was obtained with a Systronics digital conductivity meter 304 with a solute concentration of about 10^{-3} M. Electronic spectra were recorded on a Shimadzu UV 1800 (190-1100 nm) (1 cm quartz cell) spectrophotometer. ^{1}H and ^{13}C NMR spectra were obtained on a Bruker AC 400 NMR spectrometer in D_2O solution. The ESI mass spectra were recorded using a Micromass Q-Tof Micro™ (Waters) mass spectrometer. The EPR spectra were recorded on a Varian E-109C spectrometer. The room temperature magnetic susceptibilities were measured using a home built Gouy balance fitted with a polytronic DC power supply. Diamagnetic corrections for ligand susceptibilities were made using Pascal's constants.

Synthesis of the ligand

2-hydroxy-1,3-propanediamine-*N*,*N*'-dipropionic acid, H_3hpda. The precursor ligand H_3hpda was synthesized following the procedure employed for a similar ligand.[46] To a solution of β-alanine (4.455g, 50 mmol) in 30 ml water neutralized with lithium hydroxide (1.198g, 50 mmol) was added 1,3-dicholoro-2-propanol (3.223g, 25 mmol). Solid lithium hydroxide (1.198g, 50 mmol) was added in small portions to the solution with stirring while the mixture was cooled

in an ice bath. The stirring was continued at ~ 40°C for 3 days. Acidification of the solution to about pH of 5 by the addition of hydrobromic acid resulted in slight turbidity of the solution. The solution was then filtered to discard any insoluble precipitate. The clear filtrate was concentrated under vacuum until precipitation started. The mixture was kept standing at room temperature to complete the precipitation. A white precipitate was collected by filtration, washed with ethanol and diethyl ether and dried in vacuo. Yield: 7.69 g (76%). Anal. Calcd. for $C_9H_{18}N_2O_5$: C, 46.15%; H, 7.75%; N, 11.96%. Found: C, 46.23%; H, 7.87%; N, 11.89%. FTIR (cm^{-1}): ν = 3419(b), 1587(s), 1409(s), 1202(s), 1129(s), 1106(s), 1064(s), 931(s), 771(s), 614(s). ^{1}H NMR (400 MHz, D_2O, 25°C): δ 2.54-2.63 (m, 4H), 3.08-3.21 (m, 4H), 3.22-3.38 (m, 4H), 4.29-4.42 (m, 1H).

***N*,*N*'-Bis(2-pyridylmethyl)-2-hydroxy-1,3-propanediamine-*N*,*N*'-dipropionic acid, H_3phpda.** The new ligand H_3hpnda was synthesized in the final step following the procedure employed for a similar ligand.[46] To a solution of H_3hpda (2.000g, 8.538 mmol) in 20 ml water neutralized with lithium hydroxide (0.409g, 17.076 mmol) was added solid 2-picolyl chloride hydrochloride (2.801g, 17.076 mmol). Solid lithium hydroxide (0.409g, 17.076 mmol) was added in small portions with vigorous stirring while the mixture was cooled in ice bath. The stirring was continued at room temperature for 1 day, resulting in a homogeneous dark red solution. The pH of the solution was adjusted to 5 by adding hydrobromic acid. The solution was then filtered to discard any insoluble precipitate. The clear filtrate was concentrated to ~ 10 ml under vacuum and then 10 ml of ethanol was added. The reddish brown powder was precipitated by the addition of excess acetone. The product was collected by filtration, washed with acetone and recrystallized from the mixture of water, ethanol and acetone. Finally, the product was dried in vacuo. Yield: 1.99 g (73%). Anal. Calcd. for $C_{21}H_{28}N_4O_5$: C, 60.56%; H, 6.78%; N, 13.45%. Found: C, 60.59%; H, 6.71%; N, 13.52%. FTIR (cm^{-1}): ν = 3422(b), 2926(s), 1664(s), 1628(s), 1567(s), 1495(s), 1384(s). 1252(s), 1163(s), 1057(s), 893(s), 776(s), 619(s). ^{1}H NMR (400 MHz, D_2O, 25°C): δ 2.49-2.68 (m, 4H), 2.89-3.38 (m, 8H), 4.14-4.43 (m, 5H), 7.38-7.60 (m, 4H), 7.84-7.97 (m, 2H), 8.49-8.62 (m, 2H). ^{13}C NMR (400 MHz, D_2O, 25°C): 178.14, 150.00, 148.14, 140.65, 125.46, 125.10, 61.90, 57.33, 56.54, 51.97, 44.52. Mass spectrum (ESI): *m*/*z* 423 (M^+ = {H_3phpda+Li}$^+$).

Synthesis of the complexes

[Cu_2(phpda)(μ-OAc)] (1). A solution of $Cu(OAc)_2 \cdot H_2O$ (0.239 g, 1.200 mmol) in 10 ml methanol was added to a solution of H_3phpda (0.250 g, 0.600 mmol) and NaOH (0.072g, 1.800 mmol) in 15 ml methanol with magnetic stirring during a period of 10 min. The reaction mixture was then stirred for 1 h resulting a bluish green solution. The solution was filtered to discard any insoluble precipitate. The bluish green solid compound was isolated by adding excess diethyl ether to the clear filtrate. It was then filtered, washed and dried under vacuum to get the bluish green powder. Yield: 0.324 g (90%). Anal. Calcd. for $C_{23}H_{28}N_4O_7Cu_2$: C, 46.07; H, 4.71; N, 9.34; Cu, 21.20. Found: C, 46.12; H, 4.65; N, 9.39; Cu, 21.54. FTIR (cm^{-1}): ν = 3432(b), 1605(s), 1568(s), 1416(s), 1345(s), 1107(s), 1052(s), 873(s), 656(s), 621(s). Molar conductance (MeOH), Λ_M: 37 $ohm^{-1}cm^2mol^{-1}$. UV-vis spectra (H_2O) λ_{max} (ε, $M^{-1}cm^{-1}$): 704 (115), 257 (6155). Mass spectrum (ESI): *m*/*z* 672 $\{[Cu_2(phpda)(OAc)]\cdot 4H_2O+H\}^+$. Magnetic moment, μ_{eff} (tot.): 2.33 μ_B; μ_{eff}/Cu: 1.65 μ_B.

[Cu_2(phpda)(H_2O)$_2$](ClO_4) (2). A solution of $Cu(ClO_4)_2 \cdot 6H_2O$ (0.445g, 1.200 mmol) in 10 ml methanol was added to a solution of H_3phpda (0.250 g, 0.600 mmol) and NaOH (0.072g, 1.800 mmol) in 15 ml methanol with magnetic stirring during a period of 10 min. The reaction mixture was then stirred for 1 h resulting a green solution. The solution was filtered to discard the insoluble light green precipitate. The green solid compound was isolated by adding excess diethyl ether to the clear filtrate. It was then filtered, washed and dried under vacuum to get the green powder. Yield. 0.373 g (92%). Anal. Calcd. for $C_{21}H_{29}N_4O_{11}ClCu_2$: C, 37.31; H, 4.32; N, 8.29, Cu, 18.80. Found: C, 37.19; H, 4.41; N, 8.21, Cu, 18.72. FTIR (cm^{-1}): ν = 3430(b), 1609(s), 1558(s), 1429(s), 1336(s), 1088(s), 875(s), 766(s), 697(s), 627(s). Molar conductance (MeOH), Λ_M: 105 $ohm^{-1}cm^2mol^{-1}$. UV-vis spectra (H_2O) λ_{max} (ε, $M^{-1}cm^{-1}$): 706 (166), 258 (9522). Mass spectrum (ESI): *m*/*z* 659 $\{[Cu_2(phpda)(H_2O)(ClO_4)]+H\}^+$. Magnetic moment, μ_{eff} (tot.): 2.26 μ_B; μ_{eff}/Cu: 1.60 μ_B.

Catalytic hydrolysis of glycosides

In order to study the glycosidase activity of the complexes, solutions of **1** and **2** (1.0×10^{-5} M) in water at pH~10.5 (50 mM CAPS buffer) were treated separately with 100 equivalents of *p*-nitrophenyl-α-D-glucopyranoside and *p*-nitrophenyl-β-D-glucopyranoside under aerobic conditions at room temperature. Absorbance *vs* wavelength plots were recorded for these solutions at a regular time interval of 10 min in the range 365-500 nm. The reaction was monitored over the time by formation of *p*-nitrophenolate using UV-vis spectroscopy at 410 nm (ε = 16190 $M^{-1}cm^{-1}$).[50-52] The dependence of rate on substrate concentration and various kinetic parameters were determined by treating a 1.0×10^{-5} M solution of complexes **1** and **2** with different concentrations of *p*-nitrophenyl-α-D-glucopyranoside and *p*-nitrophenyl-β-D-glucopyranoside (2.0×10^{-4} M - 1.0×10^{-3} M).

DFT calculations

Theoretical calculations regarding the structure optimization, Fukui function (f_k^+) of the metal sites of complexes **1** and **2** were performed with the Gaussian 03 software.[53] The functions (f_k^+) were evaluated from single point calculations using the B3LYP[54] method and 6-311G[55] basis set at the optimized geometry, performed for N and (N+1) electron systems, where N is the total number of electrons in the system. In a finite difference approximation, f_k^+ of an atom k, in a molecule with N electrons, is expressed by the equation $f_k^+ = [q_k(N) - q_k(N+1)]$, where q_k is the charge of atom k.[56] The q_k values were calculated by Mulliken population analysis (MPA).

Acknowledgements

The authors would like to acknowledge the Council of Scientific & Industrial Research (CSIR) (Grant No.: 01(2732)/13/EMR-II), New Delhi for funding and financial support. The instrumental facilities provided by the DST-FIST and UGC-SAP program in the Department of Chemistry are greatly acknowledged. The authors acknowledge the Contingency Grant provided by the DST-PURSE program in the Department of Chemistry. A. P. also thanks the University of Kalyani for providing a university research fellowship.

Supplementary Information

Electronic supplementary information (ESI) available. See DOI: 10.1039……

Notes and References

1 B. Henrissat and A. Bairoch, *Bioche J*., 1996, **316**, 695.

2 B. Henrissat and G. Davies, *Curr. Opin. Struct. Biol.*, 1997, **7**, 637.

3 V. L. Y. Yip, J. Thompson and S. G. Withers, *Biochemistry*, 2007, **46**, 9840.

4 J. Bjerre, T. H.Fenger, L. G. Marinescu and M. Bols, *Eur. J. Org. Chem*., 2007, **4**, 704.

5 J. Bjerre, E. H. Nielsen and M. Bols, *Eur. J. Org. Chem*., 2008, **4**, 745.

6 F. Ortega-Caballero and M. Bols, *Can. J. Chem*., 2006, **84**, 650.

7 F. Ortega-Caballero, J. Bjerre, L. S. Laustsen, and M. Bols, *J. Org. Chem*., 2005, **70**, 7217.

8 F. Ortega-Caballero, C. Rousseau, B. Christensen, T. E. Petersen and M. Bols, *J. Am. Chem. Soc*., 2005, **127**, 3238.

9 C. Rousseau, N. Nielsen and M. Bols, *Tetrahedron Lett*., 2004, **45**, 8709.

10 S. H. Khan and R. A. O'Neill, *Modern methods in carbohydrate synthesis; Harwood Academic Publishers: Amsterdam, The Neterhelands*, 1996.

11 J. Baty and M. L. Sinnott, *Chem. Commun*., 2004, **7**, 866.

12 C. R. Clark, R. W. Hay and I. C. M. Dea, *J. Chem. Soc., Chem. Commun*., 1970, **13**, 794.

13 S. Striegler, N. A. Dunaway, M. G. Gichinga, J. D. Barnett and A. G. D. Nelson, *Inorg. Chem*., 2010, **49**, 2639.

14 S. Striegler, M . Dittel, R. Kanso, N. A. Alonso and E. C. Duin, *Inorg. Chem*., 2011, **50**, 8869.

15 S. Striegler, J. D. Barnett and N. A. Dunaway, *ACS Catal*., 2012, **2**, 50.

16 J. D. Barnett and S. Striegler, *Top. Catal*, 2012, **55**, 460.

17 (a) M. Bera, A. B. S Curtiss, G. T. Musie and D. R. Powell, *Inorg. Chem.*, 2012, **51**, 12093; (b) M. Bera and A. Patra, *Carbohydr. Res*., 2011, **346**, 2075; (c) M. Bera and A. Patra, *Carbohydr. Res*., 2014, **384**, 87; (d) R. A. Joy, H. Arman, S. Xian and G. T. Musie, *Inorg. Chim. Acta*, 2013, **394**, 220.

18 M. Kodera, N. Terasako, T. Kita, Y. Tachi, K. Kano, M. Yamazaki, M. Koikawa and T. Tokii, *Inorg. Chem*., 1997, **36**, 3861.

19 (a) C. H. Weng, S. C. Cheng, H. M . Wei, H. H. Wei and C. J. Lee, *Inorg. Chim. Acta*, 2006, **359**, 2029; (b) A. Mukherjee, M. K. Saha, M. Nethaji and A. R. Chakravarty, *New. J. Chem*., 2005, **29**, 596.

20 (a) D. E. Fenton, H. Okawa, *PerspectiVes on Bioinorganic Chemistry; JAI Press: London, UK*, 1993, **2**, p. 81; (b) K. D. Karlin, *Science*, 1993, **261**, 701.

21 (a) R. Breslow, *Acc. Chem. Res.*, 1991, **24**, 317; (b) A. J. Kirby, *Angew. Chem. Int. Ed. Engl.*, 1996, **35**, 707.

22 (a) D. E. Wilcox, *Chem. Rev*., 1996, **96**, 2435; (b)N. Strater, W. N. Lipscomb, T. Klabunde and B. Krebs, *Angew. Chem. Int. Ed. Engl.*, 1996, **35**, 2024.

23 W. J Geary, *Coord. Chem. Rev.,* 1971, **7***,* 81.

24 V. Zelenak, Z. Vargova and K. Gyoryova, *Spectrochim. Acta, Part A*., 2007, **66**, 262.

25 B. J. Hathaway, G. Wilkinson, R. G .Gillard and J. A .McCleverty, (*Eds*.), *Comprehensive Coordination Chemistry*., 2, Pergamon, Oxford, 1987, p. 413.

26 M. Gonzalez-Alvarez, G. Alzuet, J. Borras, S. Garcia-Granda and J. M. Montejo-Bernardo, *J. Inorg. Biochem*., 2003, **96**, 443.

27 D. Rojas, A. M. Garcia, A. Vega, Y. Moreno, D. Venegas-Yazigi, M. T. Garland and J. Manzur, *Inorg. Chem*., 2004, **43**, 6324.

28 D. Ghosh, N. Kundu, G. Maity, K. Y. Choi, A. Caneschi, A. Endo and M. Chaudhury, *Inorg. Chem*., 2004, **43**, 6015.

29 S. A. Komaei, G. A. van Albada, I. Mutikainen, U. Turpeinen and J. Reedijk, *Polyhedron*, 1999, **18**, 1991.

30 F. Zippel, F. Ahlers, R. Werner, W. Haase, H. F. Nolting and B. Krebs, *Inorg. Chem*., 1996, **35**, 3409.

31 M. G. B. Drew, P. Yates, F. S. Esho, J. Trocha-Grimshaw, A. Lavery, K. P. McKillop, S. M. Nelson and J. Nelson, *J. Chem. Soc. Dalton Trans*., 1988, 2995.

32 A. Addison, T. N. Rao, J. Reedijk, J. van Rijn and G. C. Verschoor, *J. Chem. Soc. Dalton Trans.*, 1984, 1349.

33 M. Bera, W. T. Wong, G. Aromi and D. Ray, *Eur. J. Inorg. Chem*., 2005, 2526.

34 J. D. Crane, D. E. Fenton, J. M. Latour and A. J. Smith, *J. Chem. Soc. Dalton Trans.*, 1991, 2979.

35 A. Elmali, C. T. Zeyrek and Y. Elerman. *J. Mol. Struct*., 2004, **693**, 225.

36 N. N. Murthy, K. D. Karlin, C. Berini and J. Luchinat, *J. Am. Chem. Soc*., 1997, **119**, 2156.

37 R. A. Jay, H. Arman, S. Xiang and G. T. Musie, *Inorg. Chim. Acta*, 2013, **394**, 220.

38 T. C. Lai, W. H. Chen, C. J .Lee, B. C. Wang and H. H. Wei, *J. Mol. Struct*., 2009, **935** 97.

39 Y. C. Chou, S. F. Huang, R. Koner, G. H. Lee, Y. Wang, S. Mohanta and H. H. Wei, *Inorg. Chem*., 2004, **43**, 2759.

40 V. Chandrasekhar, T. Senapati, A. Dey and E. C. Sanudo, *Inorg. Chem*., 2011, **50**, 1420.

41 Y. B. Jiang, H. Z. Kou, R. J .Wang and A. L. Cui, *Eur. J. Inorg. Chem*., 2004, 4608.

42 H. D. Bian, W. Gu, J. Y. Xu, F. Bian, S. P. Yan, D. Z. Liao, Z. H Jiang and P. Cheng, *Inorg. Chem*., 2003, **42**, 4265.

43 S. Striegler and M. G. Gichinga, *Chem. Commun*., 2008, 5930.

44 K. Selmeczi, M. Réglier, M. Giorgi and G. Speier, *Coord. Chem. Rev.*, 2003, **245**, 191.

45 S. Gupta, A. Mukherjee, M. Nethaji and A. R. Chakravarty, *Polyhedron*., 2005, **24**, 1922.

46 K. Kanamori, K. Yamamoto, T. Okayasu, N. Matsui, K. Okamoto and W. Mori, *Bull. Chem. Soc. Jpn.*, 1997, **70**, 3031.

47 M. Bera and A. Patra, *Carbohydr. Res*., 2011, **346**, 2075.

48 S. Striegler and M. J. Dittel, *Am. Chem. Soc.*, 2003, **125**, 11518.

49 S. Striegler and M. Dittel, *Inorg. Chem*., 2005, **44**, 2728.

50 Y. Lai, A. H. Bakken and J. D. Unadkat, *J. Biol. Chem.*, 2002, **277**, 37711.

51 S. W. Peretti, C. J. Tompkins, J. L. Goodall and A. S. Michaels, *J. Membr. Sci.*, 2002, **195**, 193.

52 S. E. Thompson, M. Smith, M. C. Wilkinson and K. Peek, *Appl. Environ. Microbiol.*, 2001, **67**, 4001.

53 M. J. Frisch, G. W. Trucks, H. B. Schlegel, G. E. Scuseria, M. A. Robb, J. R. Cheeseman, J. A. Montgomery, T. Vreven, Jr., K. N. Kudin, J. C. Burant, J. M. Millam, S. S. Iyengar, J. Tomasi, V. Barone, B. Mennucci, M. Cossi, G. Scalmani, N. Rega, G. A. Petersson, H. Nakatsuji, M. Hada, M. Ehara, K. Toyota, R. Fukuda, J. Hasegawa, M. Ishida, T. Nakajima, Y. Honda, O. Kitao, H. Nakai, M. Klene, X. Li, J. E. Knox, H. P. Hratchian, J. B. Cross, C. Adamo, J. Jaramillo, R. Gomperts, R. E. Stratmann, O. Yazyev, A. J. Austin, R. Cammi, C. Pomelli, J. W. Ochterski, P. Y. Ayala, K. Morokuma, G. A. Voth, P. Salvador, J. J Dannenberg, V. G Zakrzewski, S. Dapprich, A. D. Daniels, M. C Strain, O. Farkas, D. K.

Malick, A. D. Rabuck, K. Raghavachari, J. B. Foresman, J. V. Ortiz, Q. Cui, A. G. Baboul, S. Clifford, J. Cioslowski, B. B. Stefanov, G. Liu, A. Liashenko, P. Piskorz, I. Komaromi, R. L. Martin, D. J. Fox, T. Keith, M. A. Al-Laham, C. Y.; Peng, A. Nanayakkara, M. Challacombe, P. M. W. Gill, B. Johnson, W. Chen, M. W. Wong, C. Gonzalez and J. *A.* Pople, *Gaussian 03, Revision A.1; Gaussian, Inc.: Pittsburgh, PA*, 2003.

54 (a) A. D. Becke, *Phys. Rev. A*., 1988, **38**, 3098; (b) C. Lee, W. Yang and R. G. Parr, *Phys. Rev. B*., 1988, **37**, 785.

55 R. Ditchfield, W. J. Hehre and J. A. Pople, *J. Chem. Phys*., 1971, **54**, 724.

56 W. Yang and W. J. Mortier, *J. Am. Chem. Soc*., 1986, **108**, 5708.

Scheme 1 Synthesis of the ligand, H_3phpda

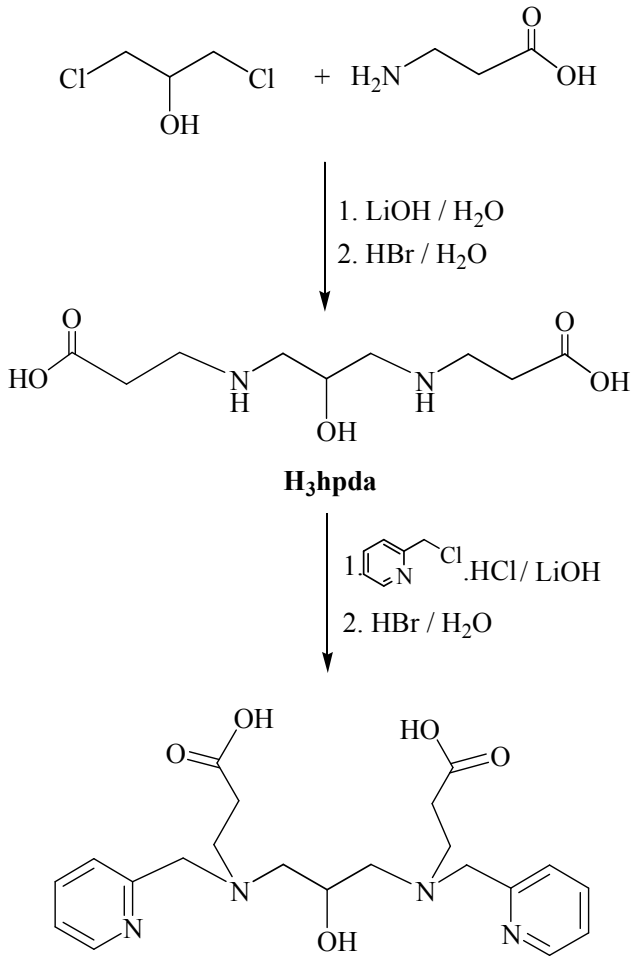

Scheme 2 Synthesis of the complexes

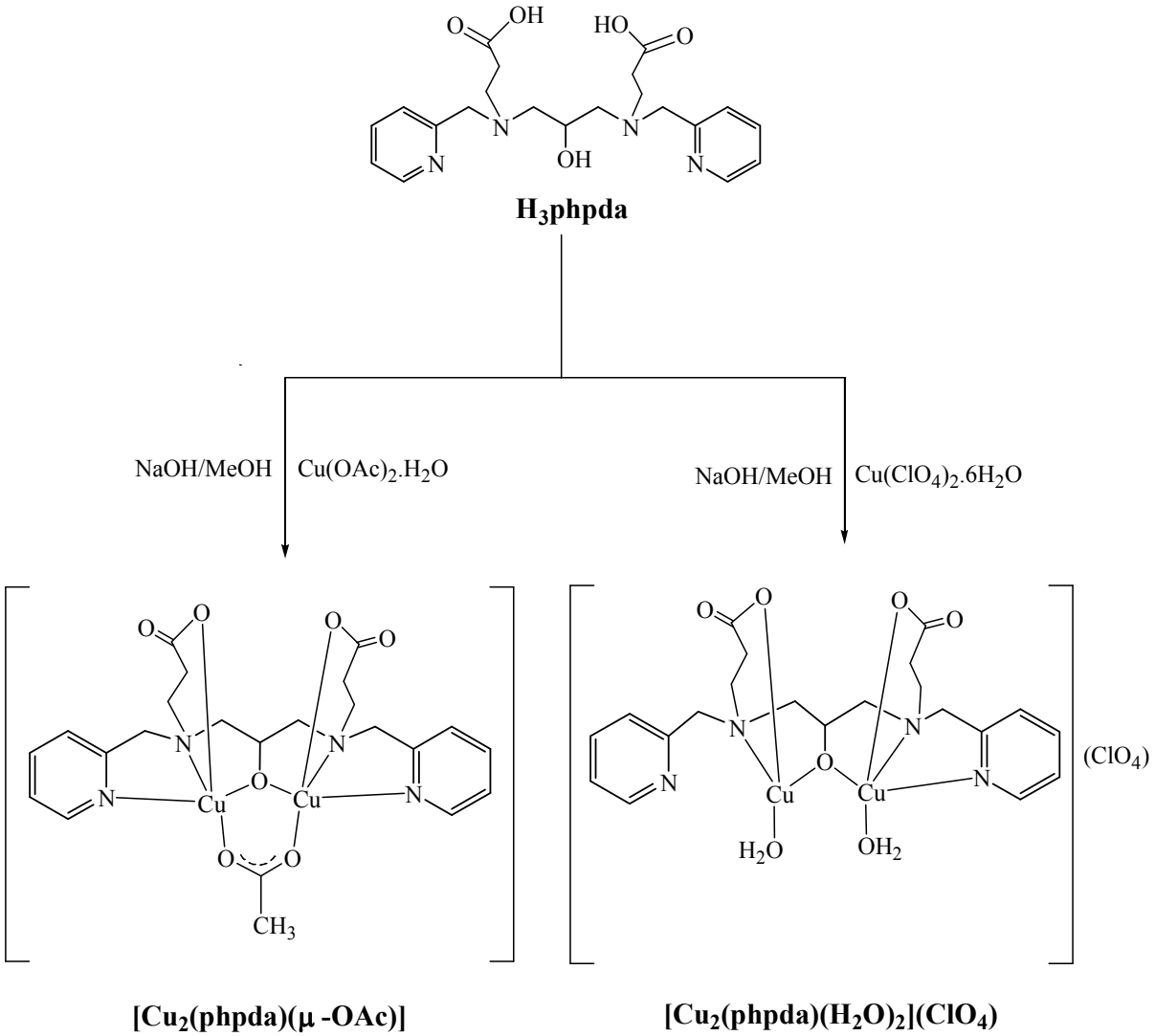

Scheme 3 Example of a glycoside hydrolysis reaction

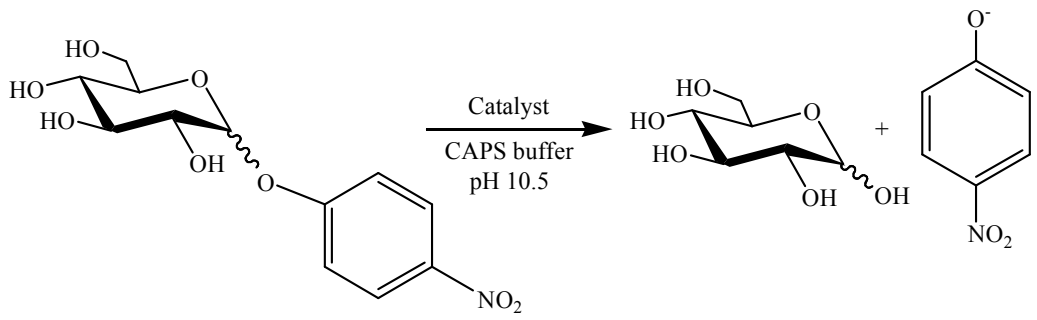

Scheme 4 Proposed mechanism for the hydrolysis of substrate **3** by complex **1**.

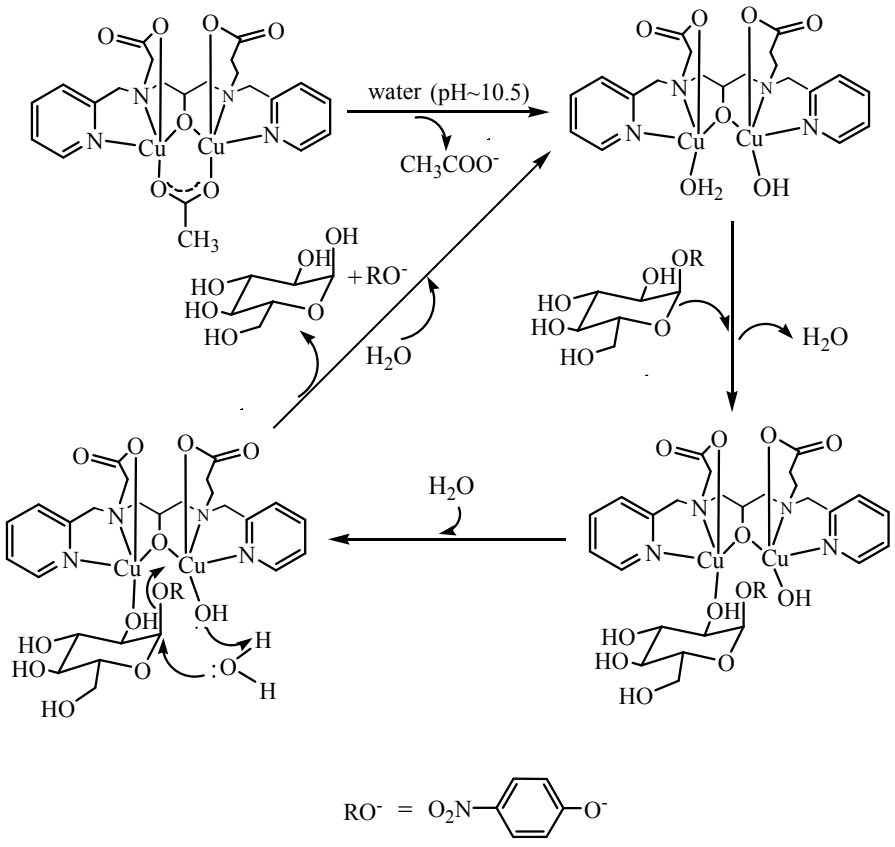

Figures with captions

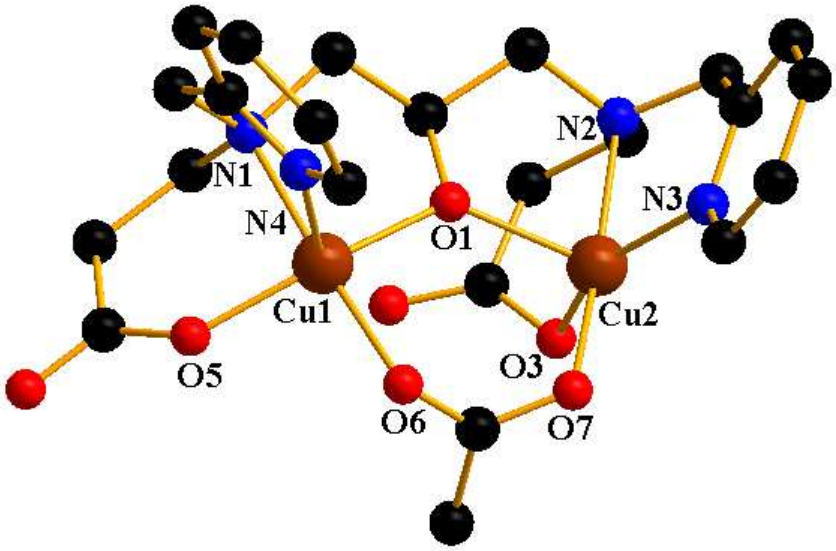

Fig. 1 DFT optimized structure of complex [Cu_2(phpda)(μ-OAc)] (**1**) with atom numbering scheme. Hydrogen atoms are omitted for clarity.

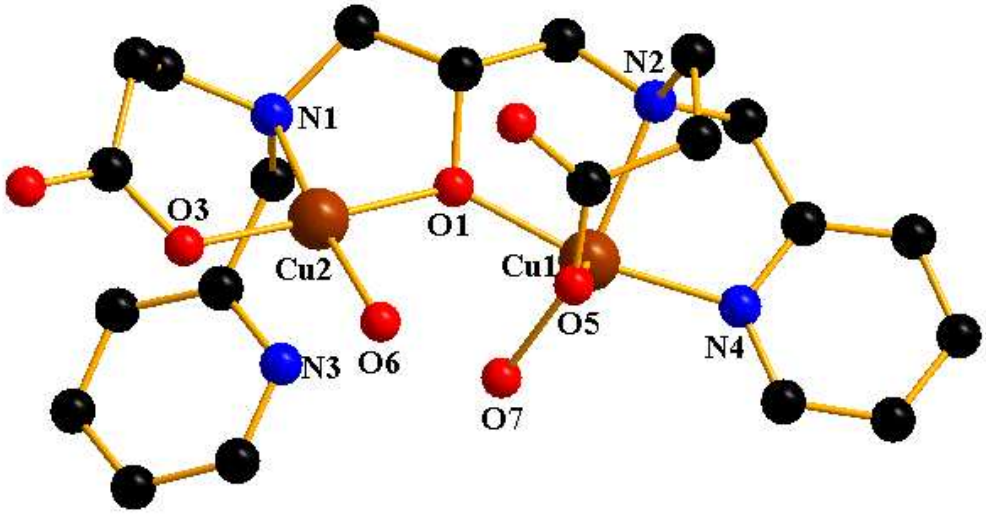

Fig. 2 DFT optimized structure of complex $[Cu_2(phpda)(H_2O)_2](ClO_4)$ (**2**) with atom numbering scheme. Hydrogen atoms are omitted for clarity.

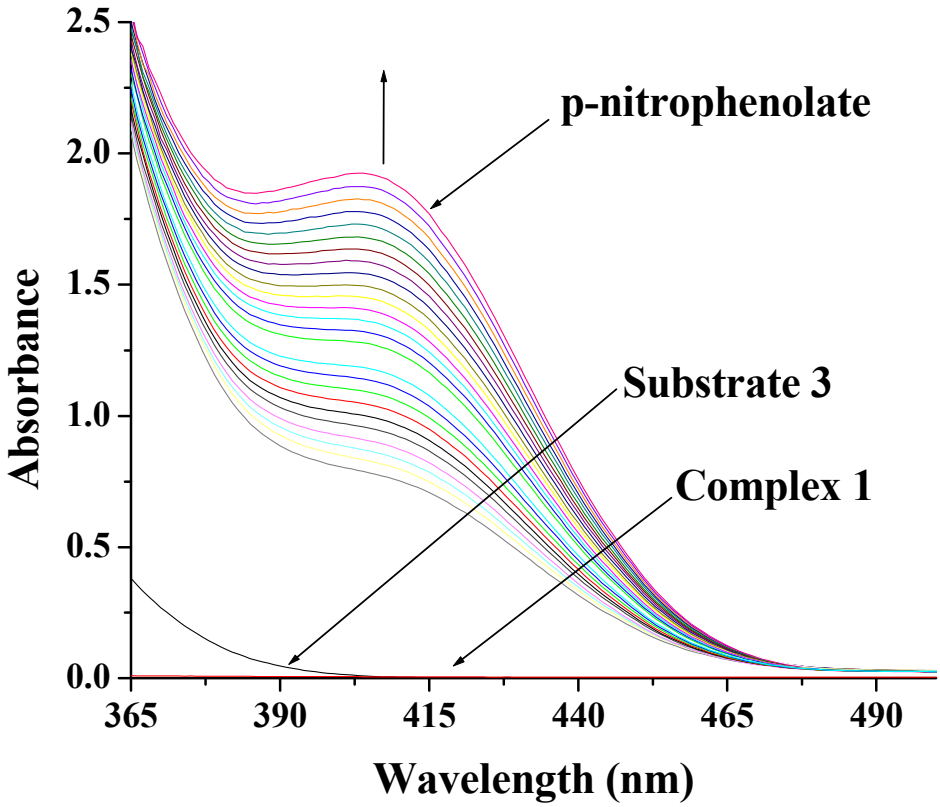

Fig. 3 UV-vis spectra (365-500 nm) of (i) complex **1** (1.0 x 10^{-5} M); (ii) *p*-nitrophenyl-α-D-glucopyranoside (**3**) (1.0 x 10^{-3} M); (iii) Changes in UV-vis spectra of complex **1** (1.0 x 10^{-5} M) upon addition of 100-fold of *p*-nitrophenyl-α-D-glucopyranoside (**3**) in aqueous solution at pH~10.5 observed after each 10 min interval.

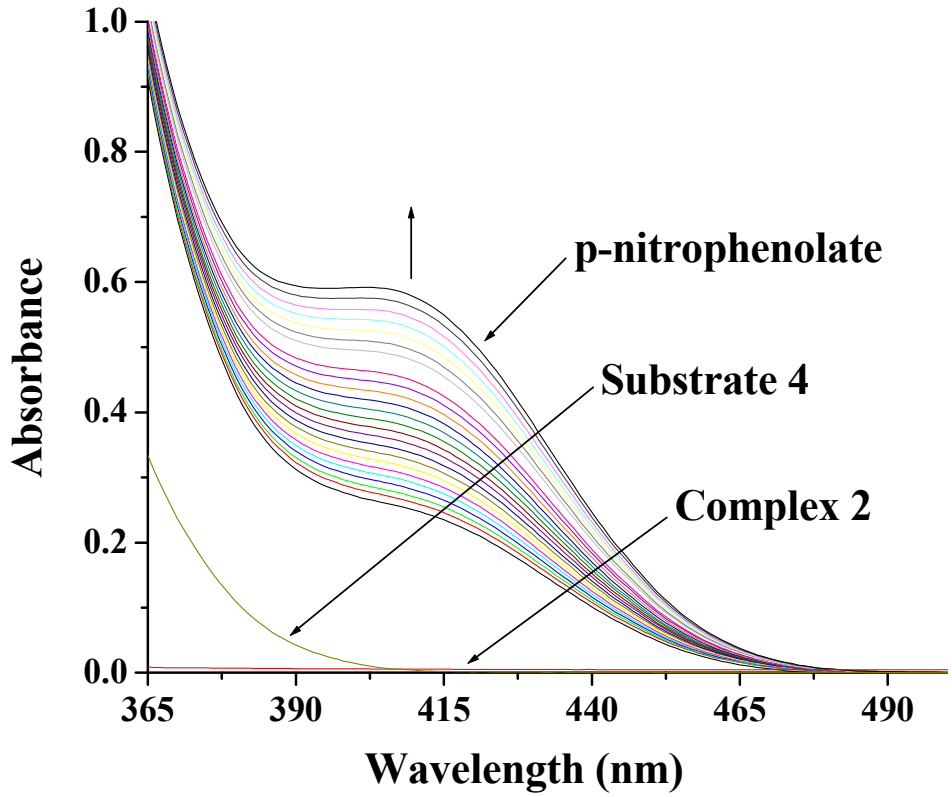

Fig. 4 UV-vis spectra (365-500 nm) of (i) complex **2** (1.0 x 10^{-5} M); (ii) *p*-nitrophenyl-β-D-glucopyranoside (**4**) (1.0 x 10^{-3} M); (iii) Changes in UV-vis spectra of complex **2** (1.0 x 10^{-5} M) upon addition of 100-fold of *p*-nitrophenyl-β-D-glucopyranoside (**4**) in aqueous solution at pH~10.5 observed after each 10 min interval.

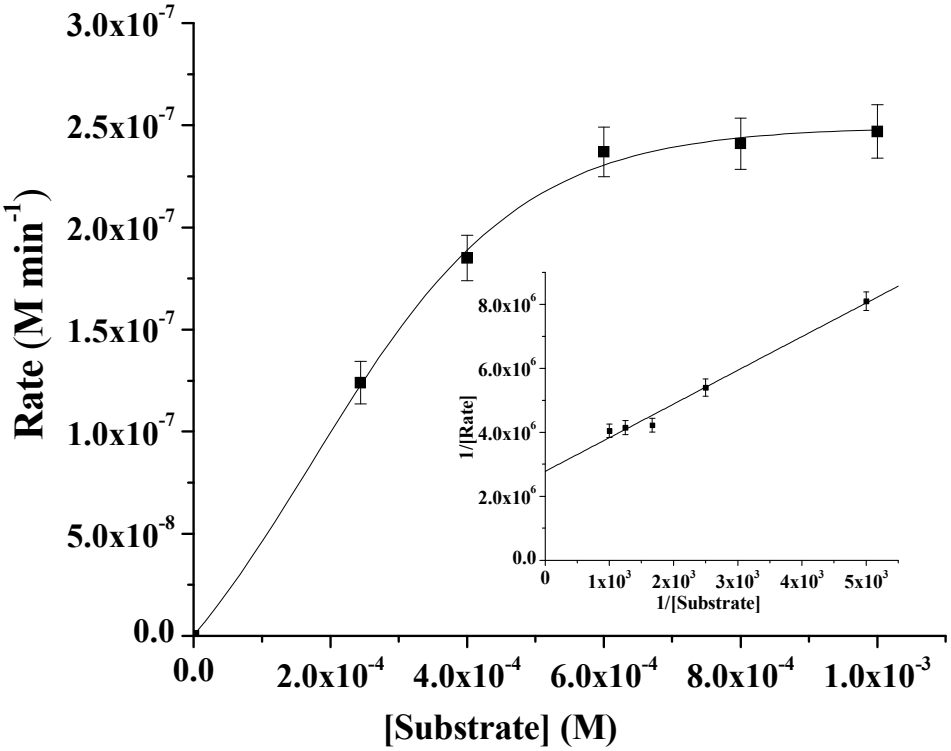

Fig. 5 Plot of rate vs. concentration of substrate **3** for complex **1**. Inset shows Lineweaver–Burk plot.

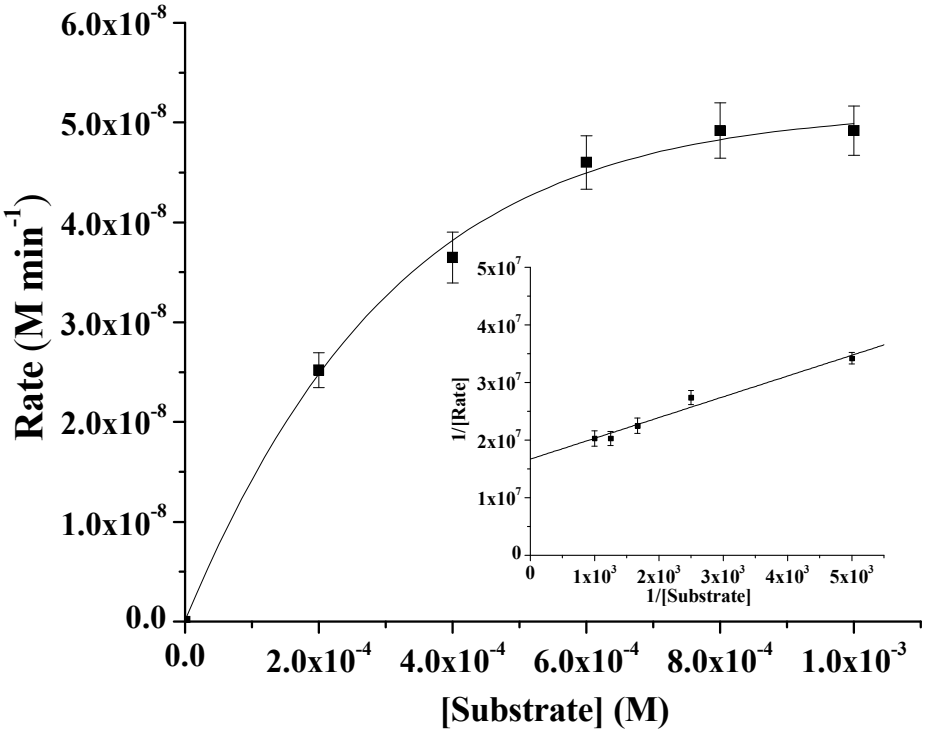

Fig. 6 Plot of rate vs. concentration of substrate **4** for complex **1**. Inset shows Lineweaver–Burk plot.

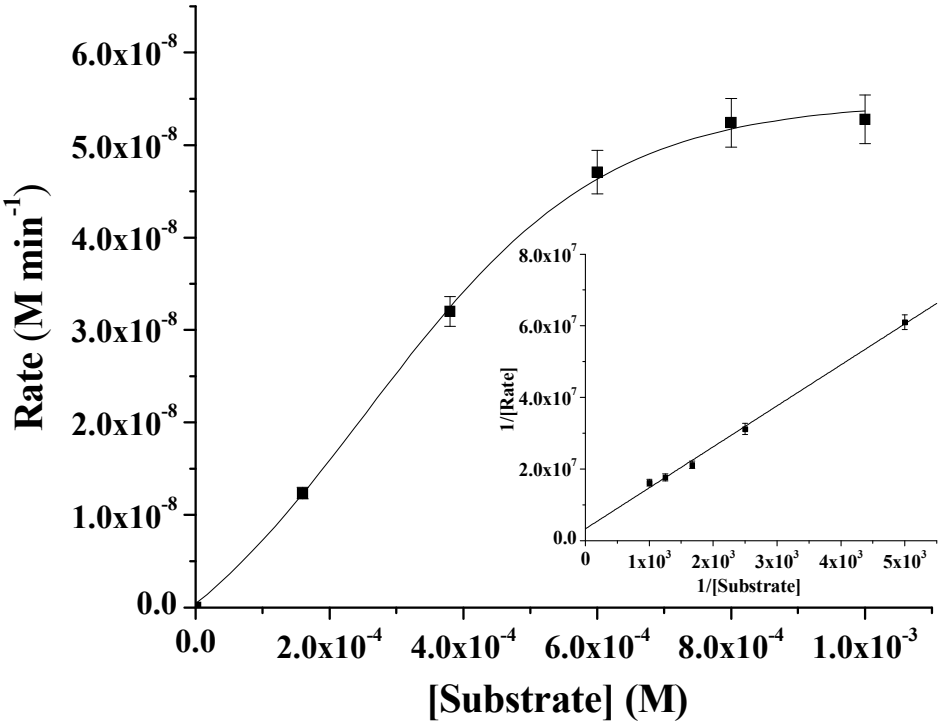

Fig. 7 Plot of rate vs. concentration of substrate **3** for complex **2**. Inset shows Lineweaver–Burk plot.

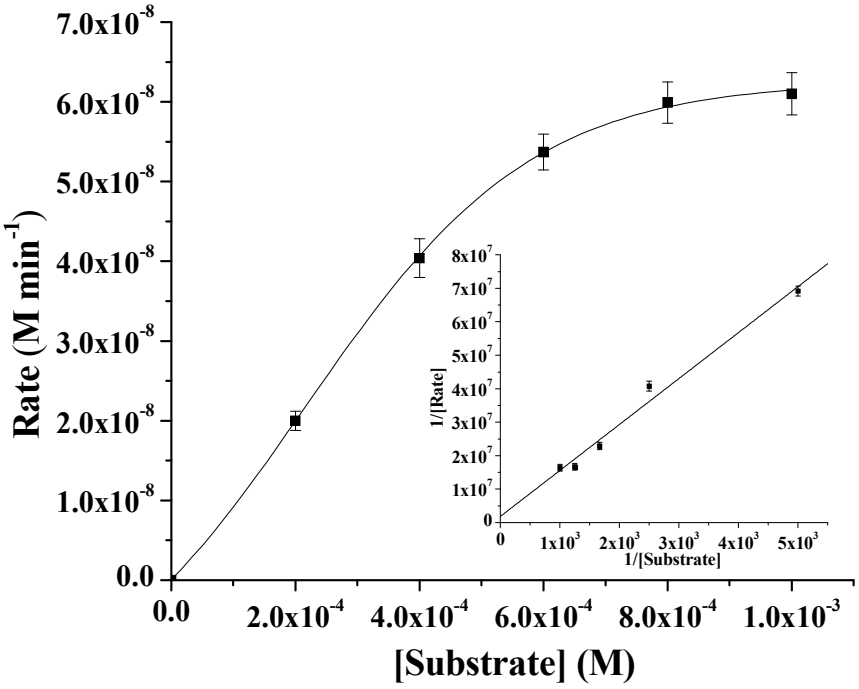

Fig. 8 Plot of rate vs. concentration of substrate **4** for complex **2**. Inset shows Lineweaver–Burk plot.

Table 1 Selected bond lengths [Å] and angles [deg] in complex **1** calculated by DFT method

Bond length [Å]

Cu(1)-O(1)	1.911	Cu(2)-O(1)	2.095
Cu(1)-O(5)	1.915	Cu(2)-O(3)	2.068
Cu(1)-O(6)	1.931	Cu(2)-O(7)	1.965
Cu(1)-N(1)	2.025	Cu(2)-N(2)	2.117
Cu(1)-N(4)	2.291	Cu(2)-N(3)	2.050

Bond angle [deg]

O(1)-Cu(1)-(O5)	163.217	O(7)-Cu(2)-N(3)	92.419
O(1)-Cu(1)-O(6)	89.776	O(7)-Cu(2)-O(3)	95.880
O(1)-Cu(1)-N(1)	86.861	O(7)-Cu(2)-O(1)	90.914
O(1)-Cu(1)-N(4)	101.943	O(7)-Cu(2)-N(2)	171.814
O(5)-Cu(1)-O(6)	92.802	N(3)-Cu(2)-O(3)	151.557
O(5)-Cu(1)-N(1)	90.513	N(3)-Cu(2)-O(1)	107.065
O(5)-Cu(1)-N(4)	93.754	N(3)-Cu(2)-N(2)	83.067
O(6)-Cu(1)-N(1)	176.622	O(3)-Cu(2)-O(1)	99.969
O(6)-Cu(1)-(N4)	101.872	O(3)-Cu(2)-N(2)	91.284
N(1)-Cu(1)-N(4)	78.544	O(1)-Cu(2)-N(2)	83.930

Table 2 Selected bond lengths [Å] and angles [deg] in complex **2** calculated by DFT method

Bond length [Å]

Cu(1)-O(1)	1.936	Cu(2)-O(3)	1.880
Cu(1)-N(4)	1.992	Cu(2)-O(1)	1.898
Cu (1)-O(7)	2.047	Cu(2)-O(6)	1.910
Cu(1)-N(2)	2.144	Cu(2)-N(1)	1.995
Cu(1)-O(5)	2.323		

Bond angle [deg]

O(1)-Cu(1)-N(4)	168.321	O(3)-Cu(2)-O(1)	178.046
O(1)-Cu(1)-O(7)	84.534	O(3)-Cu(2)-O(6)	89.548
O(1)-Cu(1)-N(2)	84.519	O(3)-Cu(2)-N(1)	98.061
O(1)-Cu(1)-O(5)	84.540	O(1)-Cu(2)-O(6)	91.423
N(4)-Cu(1)-O(7)	104.114	O(1)-Cu(2)-N(1)	81.060
N(4)-Cu(1)-N(2)	84.059	O(6)-Cu(2)-N(1)	171.848
N(4)-Cu(1)-O(5)	99.944		
O(7)-Cu(1)-N(2)	148.534		
O(7)-Cu(1)-O(5)	107.695		
N(2)-Cu(1)-O(5)	100.499		

Table 3 Kinetic parameters for complexes **1** and **2**

Complex	Substrate	K_{cat} x 10^{-3} (min^{-1})	K_m x 10^{-6} (M)	V_{max} x 10^{-8} (M min^{-1})	K_{cat}/K_m ($M^{-1}min^{-1}$)	K_{non} x 10^{-7} ($M^{-1}min^{-1}$)[a]
1	3	33.0 ± 0.3	347.1 ± 18.2	33.0 ± 0.3	95.1	2.8
2	3	29.9 ± 1.7	3419.6 ± 32.1	29.9 ± 1.7	8.7	2.8
1	4	8.6 ± 0.5	308.6 ± 1.5	8.5 ± 0.5	27.7	2.2
2	4	53.7 ± 3.0	7365.7 ± 4.4	53.6 ± 3.0	7.3	2.2

[a]Data has been taken from ref 13.

Table 4 Fukui functions of complexes **1** and **2**

Complex	**1**		**2**	
Atom	Cu(1)	Cu(2)	Cu(1)	Cu(2)
f_k^+	0.0167	0.0970	0.1739	0.0147